Report

Cell Reports

Vulnerability of Purkinje Cells Generated from Spinocerebellar Ataxia Type 6 Patient-Derived iPSCs

Graphical Abstract

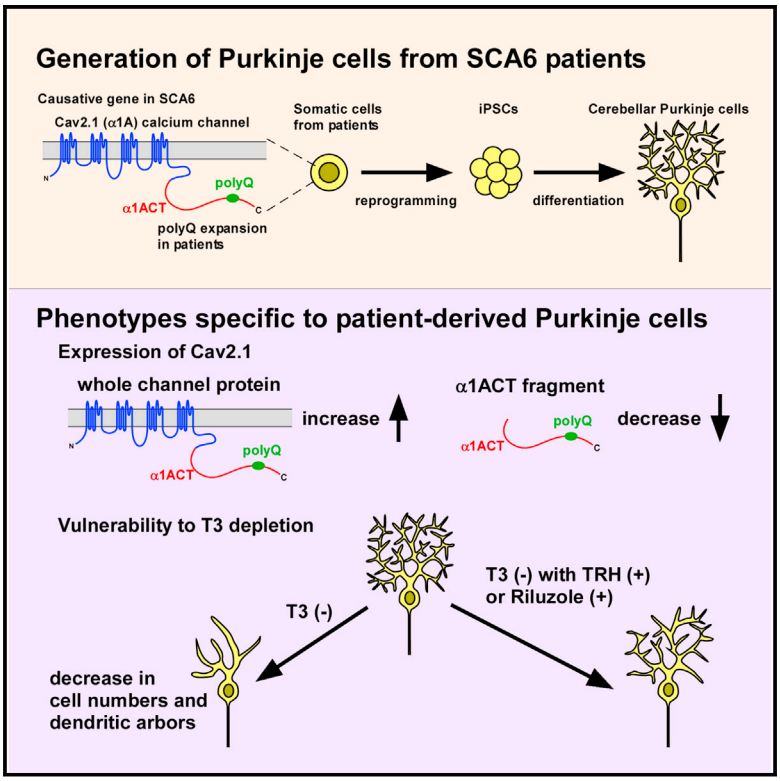

Highlights

- Purkinje cells are generated from SCA6 patient-derived iPSCs
- Patient cells show increased full-length Cav2.1, but decreased C-terminal fragment
- T3 depletion causes decrease in cell number and dendritic arbors in patient cells
- T3 depletion-induced degeneration was suppressed by treatment with TRH or Riluzole

Authors

Yoshihito Ishida, Hideshi Kawakami, Hiroyuki Kitajima, Ayaka Nishiyama, Yoshiki Sasai, Haruhisa Inoue, Keiko Muguruma

Correspondence

muguruma@cdb.riken.jp

In Brief

Ishida et al. generated cerebellar Purkinje cells from spinocerebellar ataxia 6 patient-derived iPSCs. They demonstrate that patient-derived Purkinje cells show vulnerability to triiodothyronine depletion, which is suppressed by treatment with thyrotropin-releasing hormone and Riluzole. This in vitro disease model will be useful for pathogenic investigation and drug screening.

Accession Numbers

GSE85347
GSE85348

Ishida et al., 2016, Cell Reports *17*, 1482–1490
November 1, 2016
http://dx.doi.org/10.1016/j.celrep.2016.10.026

OPEN ACCESS
CellPress

Cell Reports
Report

Vulnerability of Purkinje Cells Generated from Spinocerebellar Ataxia Type 6 Patient-Derived iPSCs

Yoshihito Ishida,[1,2,3] Hideshi Kawakami,[4] Hiroyuki Kitajima,[1] Ayaka Nishiyama,[2] Yoshiki Sasai,[1,6] Haruhisa Inoue,[5] and Keiko Muguruma[1,2,7,*]

[1]Laboratory for Organogenesis and Neurogenesis
[2]Laboratory for Cell Asymmetry
RIKEN Center for Developmental Biology, Kobe 650-0047, Japan
[3]Drug Discovery & Disease Research Laboratory, Shionogi & Co., Ltd., Osaka 561-0825, Japan
[4]Department of Epidemiology, Research Institute for Radiation Biology and Medicine, Hiroshima University, Hiroshima 734-8553, Japan
[5]Department of Cell Growth and Differentiation, Center for iPS Cell Research and Application, Kyoto University, Kyoto 606-8507, Japan
[6]Deceased August 5, 2014
[7]Lead Contact
*Correspondence: muguruma@cdb.riken.jp
http://dx.doi.org/10.1016/j.celrep.2016.10.026

SUMMARY

Spinocerebellar ataxia type 6 (SCA6) is a dominantly inherited neurodegenerative disease characterized by loss of Purkinje cells in the cerebellum. SCA6 is caused by CAG trinucleotide repeat expansion in *CACNA1A*, which encodes Cav2.1, α1A subunit of P/Q-type calcium channel. However, the pathogenic mechanism and effective therapeutic treatments are still unknown. Here, we have succeeded in generating differentiated Purkinje cells that carry patient genes by combining disease-specific iPSCs and self-organizing culture technologies. Patient-derived Purkinje cells exhibit increased levels of full-length Cav2.1 protein but decreased levels of its C-terminal fragment and downregulation of the transcriptional targets TAF1 and BTG1. We further demonstrate that SCA6 Purkinje cells exhibit thyroid hormone depletion-dependent degeneration, which can be suppressed by two compounds, thyroid releasing hormone and Riluzole. Thus, we have constructed an in vitro disease model recapitulating both ontogenesis and pathogenesis. This model may be useful for pathogenic investigation and drug screening.

INTRODUCTION

Spinocerebellar ataxia (SCA) is a group of hereditary ataxic neurodegenerative disorders without effective treatment or cure. The patients progressively lose physical control while retaining full mental capacity. SCA6 is an autosomal-dominant disease characterized by the loss of Purkinje cells, the sole output neurons of the cerebellar cortex (Matilla-Dueñas et al., 2014; Leto et al., 2015). SCA6 is caused by expansion of polyglutamine (polyQ)-encoding CAG trinucleotide repeat in *CACNA1A*, which encodes Cav2.1, α1A subunit of P/Q-type calcium channel (Zhuchenko et al., 1997; Ishikawa et al., 1997; Matsuyama et al., 1997). The numbers of the repeat are 8–14 in healthy controls, but 20–23 in the patients (Rüb et al., 2013). Patient Purkinje cells show an abnormal morphology with irregularly shaped nuclei and swelling of dendritic arbors (Yang et al., 2000). Despite accumulating information, the pathogenic mechanisms and effective therapeutic treatments are still unknown. To date, several animal models and human cell line models have been reported (Rüb et al., 2013), but whether they recapitulate the human disease phenotypes cannot be guaranteed (Watson et al., 2015). Here, to construct an in vitro disease model, we developed a strategy to generate differentiated human Purkinje cells that carry SCA6 patient genes. We combined the techniques for generation of induced pluripotent stem cells (iPSCs) from patients (Takahashi et al., 2007) with those for differentiation of human PSCs into cerebellar tissues and Purkinje cells (Muguruma et al., 2015) through recapitulation of ontogenesis by the self-organizing activity (Sasai, 2013).

With these patient-derived Purkinje cells, we first investigated the distribution pattern of Cav2.1 protein and its C-terminal domain (α1ACT), and found increased level of whole Cav2.1 protein while decreased level of α1ACT. We next found vulnerability to depletion of the thyroid hormone triiodothyronine (T3) in SCA6 Purkinje cells. Finally, we demonstrated that two compounds, thyrotropin-releasing hormone (TRH) and Riluzole suppressed the vulnerability. Thus, we succeeded in construction of an in vitro disease model of SCA6 for pathogenic investigation and drug discovery.

RESULTS

Generation of Purkinje Cells from SCA6 Patient-Derived iPSCs

Dermal fibroblasts (DF) from two independent SCA6 patients (SCD166 with heterozygous allele and SCD162 with homozygous alleles for expanded CAG repeats) and peripheral blood

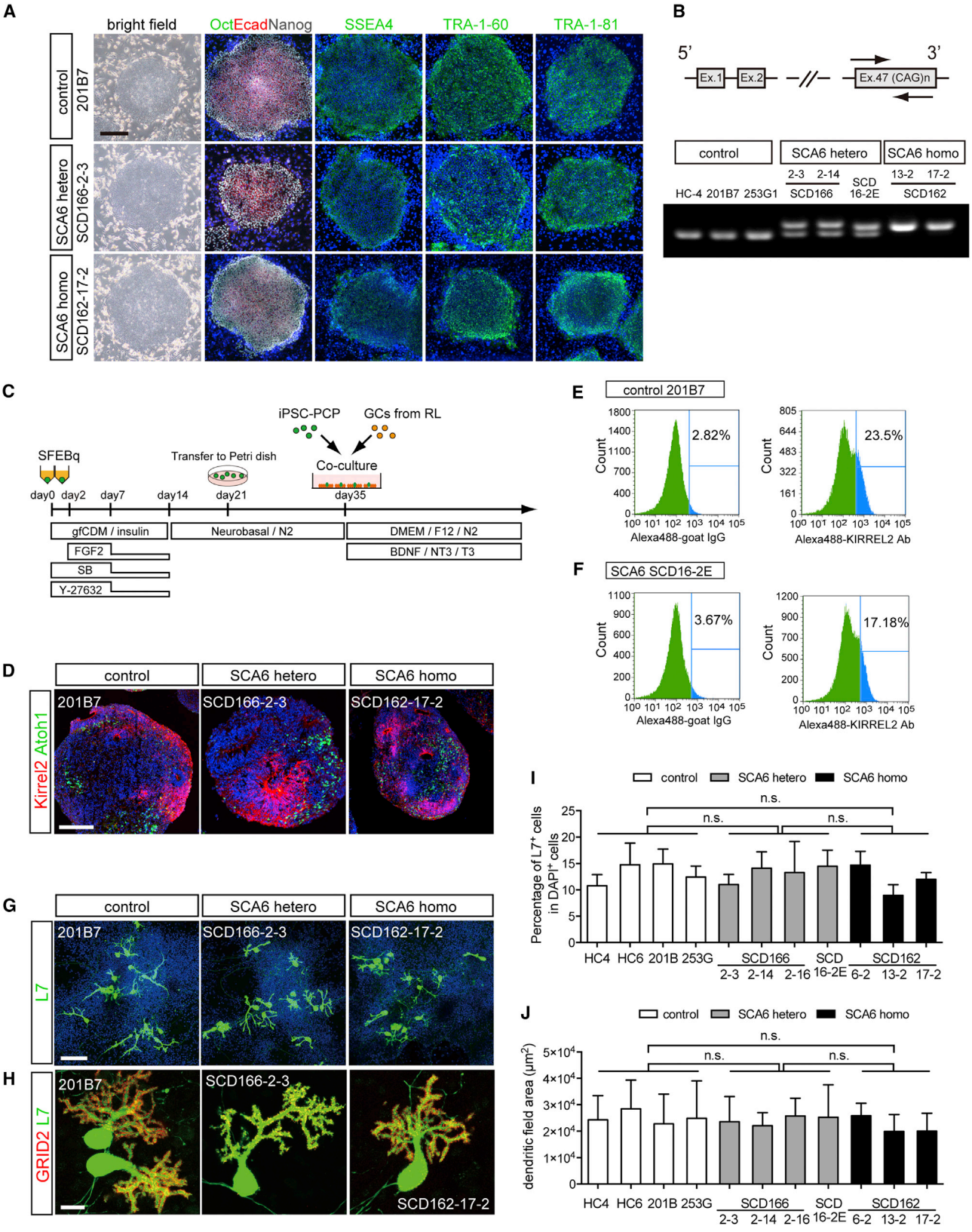

(legend on next page)

mononuclear cells (PBMCs) from a heterozygous patient (SCD16) and two healthy donors (HC-4 and HC-6) were reprogrammed by episomal vectors (Table S1) (Nakagawa et al., 2008; Okita et al., 2011, 2013). Both healthy donor-derived control iPSC clones (including additional clones 201B7 and 253G1) (Takahashi et al., 2007; Nakagawa et al., 2008) and patient-derived iPSC clones similarly showed human embryonic stem cell (hESC)-like morphology and marker expression patterns (Figures 1A and S1A), normal karyotype (Figure S1B), and expression pattern of global and PSC-related genes (Figures S1C–S1F). SCA6 iPSCs carried expanded CAG repeats (more than 21), while control iPSCs did normal repeats (around 11) (Figures 1B, S1G, and S1H). Thus, control and SCA6 clones share characteristics of iPSCs, while maintaining the original length of CAG repeats within *CACNA1A* (Figures 1B and S1G–S1I). These iPSCs were differentiated into cerebellar neurons as previously described (Muguruma et al., 2015; Morino et al., 2015) with some modifications (Figure 1C). On day 35 in culture, iPSC aggregates came to express the Purkinje cell progenitor marker KIRREL2, the granule cell (GC) precursor marker ATOH1, and the neuronal marker MAP2 in a spatially distinct manner (Figures 1D, S1J, and S1K). At this stage, KIRREL2$^+$ Purkinje progenitors were purified by fluorescence-activated cell sorting (FACS) (Figures 1E and 1F). The percentages of KIRREL2$^+$ cells in FACS analysis on day 35 were 21.8%–34.7% for control cells (n = 3) and 16.3%–23.5% for SCA6-derived cells (n = 3). They did not show large variability between the cell lines and were within the range for human ESCs (Muguruma et al., 2015). The purified progenitors were further differentiated into Purkinje cells in the co-culture with GCs derived from upper rhombic lip (Muguruma et al., 2010, 2015) (Figure 1C). Both control and SCA6 progenitors came to express the early Purkinje cell marker LHX5 on day 45 (Figure S1L) and Purkinje cell-specific marker L7/PCP2 on day 49 (Figures 1G and S1M). After long-term culture (>70 days), L7$^+$ Purkinje cells extended elaborate dendritic arbors and dendritic spines positive for Purkinje cell-specific glutamate receptor GRID2 (Figures 1H and S1N). No significant differences were observed between SCA6 and control L7$^+$ cells in frequency (Figure 1I), dendritic field area (Figure 1J), total length of dendrites (Figure S1O), or soma diameter (Figure S1P). Thus, we established an efficient method to generate differentiated Purkinje cells that carry genes of SCA6 patients.

Cav2.1 Protein Is Upregulated in SCA6 Purkinje Cells

Cav2.1, the protein product of *CACNA1A*, is expressed in the cell body and dendrites of mature Purkinje cells (Westenbroek et al., 1995; Craig et al., 1998; Indriati et al., 2013). Cytoplasmic aggregation of Cav2.1 was observed in Purkinje cells of SCA6 patients (Ishikawa et al., 1999). We confirmed these previous findings in patient Purkinje cells. In control cultures on days 75–80, Cav2.1 was expressed as puncta uniformly distributed throughout the L7$^+$ Purkinje cells (Figures 2A and S2A). A similar pattern was found in SCA6 Purkinje cells (Figures 2B, 2C, S2B, and S2C). However, Cav2.1 signals in SCA6 Purkinje cells were higher than those in control cells (Figures 2A–2C). The signal levels both in dendrites and soma did not vary among the cell lines within the same (control, heterozygous, or homozygous) group, but varied among the groups (Figures 2D and 2E). They increased as the number of allele with expanded CAG repeats increased. These results indicate that the Cav2.1 protein level is correlated with the gene dosage. We analyzed global gene expression profile on iPSC-derived Purkinje progenitors on day 35 (Figure S2D). At this rather immature stage, homozygote/control ratio of *CACNA1A* mRNA level was 0.95.

C-Terminal Domain of Cav2.1 Is Decreased in SCA6 Purkinje Cells

Evidence suggests that the C-terminal fragment of Cav2.1 (α1ACT) harboring the polyQ tract is involved in the pathology of Purkinje cells (Kordasiewicz et al., 2006; Du et al., 2013). α1ACT is translated from the bicistronic transcript, conveyed to the nucleus, and functions as a transcription factor for TAF1 and BTG1 (Figure 3A) (Du et al., 2013). α1ACT with expanded polyQ tract exhibits neuronal toxicity depending on the length (Kordasiewicz et al., 2006; Du et al., 2013). We examined α1ACT expression with a specific antibody (against 2225–2314 amino acids in human) in Purkinje cells on days 75–80 (Figures 3 and S3). In control cells, punctate signals were observed in the nucleus, but not in the dendrites (Figures 3B, 3E, S3A, and S3D). Signals were also observed in SCA6 Purkinje cells (Figures 3C, 3D, 3F, 3G, S3B, S3C, S3E, and S3F), but their level was lower (Figures 3B–3G and S3A–S3F). In an opposite manner to the whole Cav2.1 protein (Figure 2), signal level of α1ACT was negatively correlated with the gene dosage (Figure 3H). TAF1 (Figures 3B–3D and S3A–S3C) and BTG1 (Figures 3E–3G and S3D–S3F) show similar dependency of signal level on the gene dosage (Figures 3I and 3J). Similar gene dosage dependency was also detected for both mRNAs by qPCR analysis (Figures 3K and 3L). In contrast, the global gene expression analysis revealed that none of the target genes (*TAF1*, *BTG1*, *ATP2B2*, or *GRN*) differed between control and SCA6 Purkinje progenitors on day 35 (Figure S2D), indicating that the differential expression had not yet occurred at this rather immature stage. These results

Figure 1. Generation of Differentiated Purkinje Cells from SCA6 iPSCs

(A) Morphology and marker expression pattern of iPSC clones derived from a healthy donor (201B7), heterozygous (SCD166-2-3), and homozygous (SCD162-17-2) patients.

(B) PCR of CAG repeats containing exon 47 of *CACNA1A* (top) amplified fragments of different sizes depending on the number of CAG repeats (bottom).

(C) Protocol for differentiation of Purkinje cells from iPSCs (see Supplemental Experimental Procedures). PCP, Purkinje cell progenitor; GC, granule cell.

(D) Immunostaining of iPSC aggregates on day 35.

(E and F) FACS analysis of KIRREL2$^+$ cells in SCA6− (SCD16-2E, n = 3) and control (201B7, n = 3) iPSC aggregates on day 35.

(G and H) Immunostaining of Purkinje cells on days 49 (G) and 75–80 (H).

(I and J) Percentage (I) and dendritic field area (J) of L7$^+$ cells in cultures on days 70–80.

Each bar represents mean ± SD from independent experiments (n ≥ 3). The scale bars represent 500 μm (A), 200 μm (D), 100 μm (G), and 20 μm (H). n.s., not significant. See also Figure S1 and Table S1.

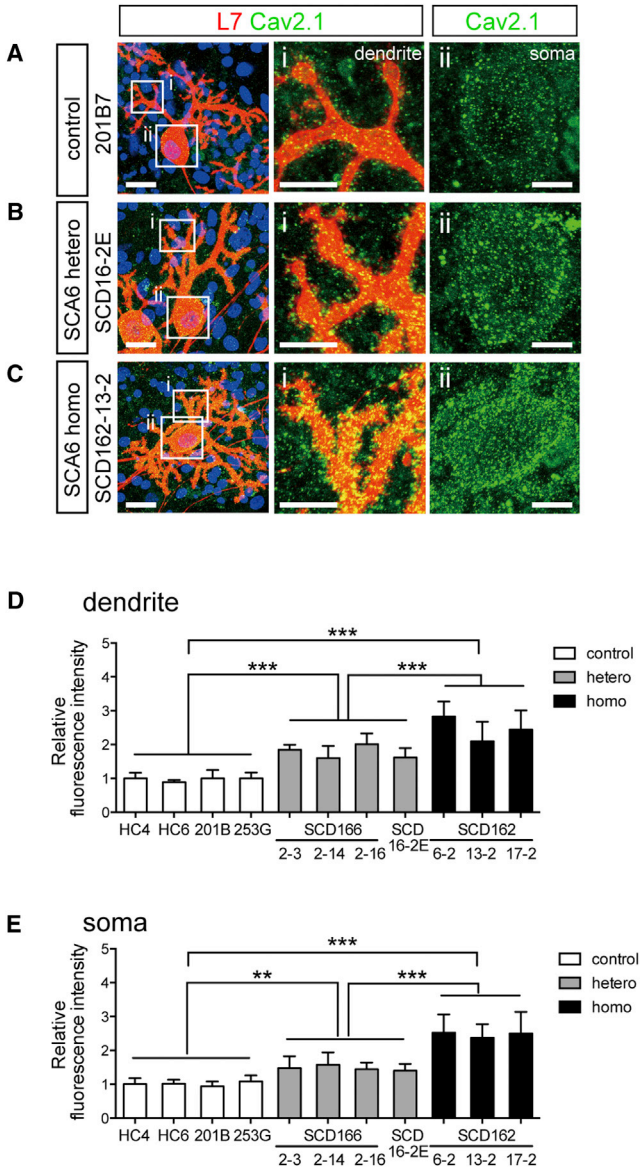

Figure 2. Elevated Level of Cav2.1 Protein in SCA6 Purkinje Cells

(A–C) Immunostaining of Purkinje cells derived from control (201B7) (A), heterozygous (SCD16-2E) (B), and homozygous (SCD162-13-2) (C) iPSCs on days 75–80 for Cav2.1 (green) and L7 (red). The insets in the left columns were magnified in the middle and the right columns. The scale bars represent 20 μm (left) and 10 μm (middle and right).

(D and E) Relative fluorescence intensity of Cav2.1 normalized with the average of control values in soma (D) and dendrites (E).

Each bar represents mean ± SD from independent experiments ($n \geq 3$). **$p < 0.01$ and ***$p < 0.001$. See also Figure S2.

indicate that the level of α1ACT and its target proteins are decreased in SCA6 Purkinje cells in correlation with the gene dosage. The findings are consistent with the notion that the expanded polyQ tract in Cav2.1 has a negative effect on the development, maturation, or survival of Purkinje cells through the suppression of transcriptional activity of α1ACT (Du et al., 2013).

SCA6 Purkinje Cells Show Vulnerability to Nutrient Depletion

As described above, it is important to confirm whether the previous findings are also found in the iPSC-derived Purkinje cells. However, the greatest advantage of using patient Purkinje cells lies in the identification of as-yet-unknown patient-specific phenotypes before the disease onset. An exploration of in vitro disease phenotypes would be the basis for the mechanistic investigation of pathogenesis and for drug discovery in the future (Inoue et al., 2014; Watson et al., 2015). In this direction, we searched for pathological phenotypes that would signify the difference between control and SCA6 Purkinje cells. It is known that maturation and maintenance of Purkinje cells is supported by thyroid hormone T3 (Heuer and Mason, 2003; Leto et al., 2015), which is included in the cerebellar maturation media (Muguruma et al., 2015). Thus, we imposed strict culture conditions on differentiated Purkinje cells by depletion of T3 (Figure 4A). Depletion for 5 days from day 70 did not exert apparent effects on control cells (compare "none" and "vehicle" columns in Figure S4A), but caused loss of SCA6 cells (none and vehicle in Figures S4B and S4C). The number of survived cells did not differ between the presence and absence of T3 in Purkinje cells derived from two control lines (none and vehicle in Figures 4B and S4D). In contrast, the numbers decreased in T3-depleted cultures of Purkinje cells derived from two heterozygous (Figures 4C and S4E) and two homozygous (Figures 4D and S4F) lines. Numbers of heterozygous and homozygous cells were smaller than those of control cells (column "V" in Figures 4E and S4G).

We further noticed that the surviving SCA6 cells bore thickened dendrites with poor arborization (none and vehicle in Figures 4F–4H). Dendritic field areas of control cells did not differ between the presence and absence of T3 (none and vehicle in Figures 4I and S4H), but those of heterozygous (Figures 4J and S4I) and homozygous (Figures 4K and S4J) cells decreased by T3 depletion. Dendritic field areas of heterozygous and homozygous cells were smaller than those of control cells (column V in Figures 4L and S4K). These results indicate that T3 depletion caused vulnerability specifically to patient Purkinje cells.

The Vulnerability of SCA6 Purkinje Cells Is Blocked by Thyroid Releasing Hormone and Riluzole

We further explored compounds that improve the vulnerability of SCA6 Purkinje cells to evaluate whether this culture system could be used as an assay system for drug discovery. We tested several candidate compounds in T3-depleted cultures (Figures 4 and S4). Among them, TRH, which has been used for treatment to SCA6 patients, enhanced the survival (Figures 4B–4E and S4B–S4G) and dendritic maintenance of SCA6 Purkinje cells (Figures 4G–4L and S4I–S4K). Another effective compound was Riluzole (Figures 4B–4H), which is a drug used to treat amyotrophic lateral sclerosis (ALS). Other compounds, including SAG, a hedgehog pathway agonist supporting cell survival, and Y-27632, a ROCK inhibitor associated with stability of dendrites, did not show improvement (Figures 4B–4L and S4B–S4L).

Response of SCA6 Purkinje Cells to Cellular Stress

An autophagy marker LC3 was highly expressed in SCA6 cells (Figure S4M), which is consistent with a previous report (Unno

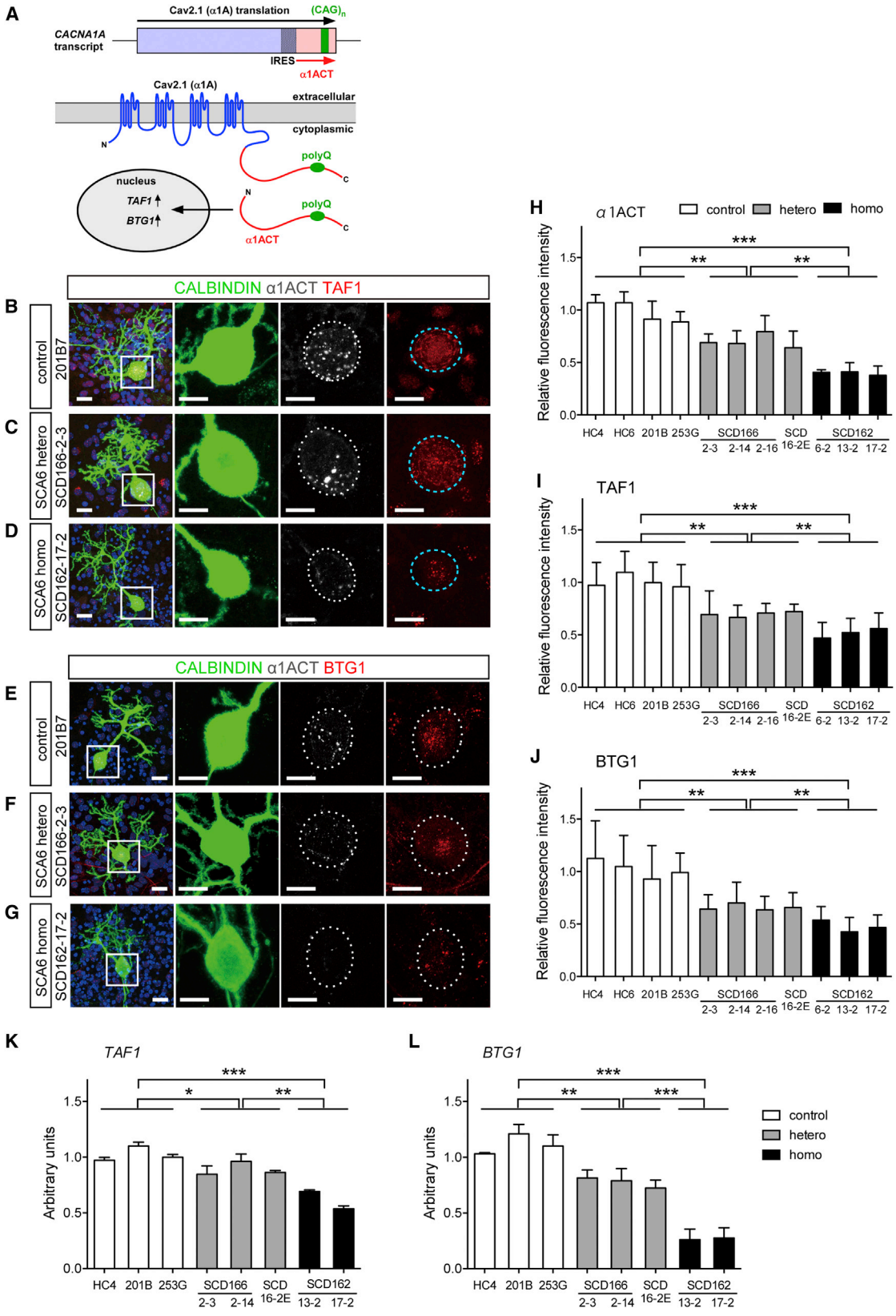

(legend on next page)

et al., 2012). We further tested responses to various cellular stresses. Tunicamycin, an endoplasmic reticulum stress inducer, did not show apparent effects (Figure S4N). Bafilomycin, a V-ATPase inhibitor, but not MG132, a proteasome inhibitor, selectively decreased the number of SCA6 cells (Figures S4O and S4P).

DISCUSSION

Construction of In Vitro SCA6 Models with Patient-Derived iPSCs

Investigation of SCAs has long been hampered by unavailability of living human Purkinje cells, which degenerate in SCA patients (Watson et al., 2015). Alternatively, several animal models and human cell line models have been developed (Rüb et al., 2013), but it is uncertain whether these models recapitulate the disease phenotypes. Recent iPSC technologies offer an opportunity to use patient-derived neurons that carry disease-specific genes (Inoue et al., 2014). Simple cellular models with iPSC-derived neurons certainly brought important information (Koch et al., 2011), but they still have a limitation in studying late-onset SCAs because degeneration occurs in mature Purkinje cells. We have recently developed an efficient method for generation of differentiated Purkinje cells from human PSCs (Muguruma et al., 2015), utilizing 3D self-organizing principles (Sasai, 2013). This study, by combining the patient-derived iPSC technology and the self-organizing stem cell culture technology, has succeeded in generation of SCA6 patient-derived Purkinje cells. The patient-derived Purkinje cells can be used for construction of in vitro disease models for SCA6.

Recapitulation of the Disease Phenotypes in Patient-Derived Purkinje Cells

We confirmed that Cav2.1 was expressed in the cell body and dendrites of both control and patient Purkinje cells, as reported in the rat (Westenbroek et al., 1995; Craig et al., 1998; Indriati et al., 2013) and human postmortem tissues (Ishikawa et al., 1999). Ishikawa et al. (1999) observed that Purkinje cells of SCA6 patients show cytoplasmic aggregation of Cav2.1 in the peripheral perikarya and the proximal dendrites and its reduced expression in the distal dendrites. We found that the level of Cav2.1 protein was increased as the gene dosage increased (Figures 2 and S2). However, the spatial distribution pattern of Cav2.1 was similar among the groups. Cav2.1 was uniformly expressed as puncta distributed throughout the cells. Such discrepancy could be due to the difference in stages of maturation between still-growing rather immature iPSC-derived cells and dying mature cells.

Evidence suggests that α1ACT, bicistronically translated Cav2.1 C-terminal fragment harboring the polyQ tract, is involved in the pathology of Purkinje cells (Kordasiewicz et al., 2006; Du et al., 2013; Miyazaki et al., 2016). α1ACT fragment is conveyed to the nucleus and functions as a transcription factor for TAF1 and BTG1 (Du et al., 2013). α1ACT exhibits neuronal toxicity depending on the length of polyQ tract (Kordasiewicz et al., 2006; Du et al., 2013). In this study, we found that α1ACT was detected as puncta in the nucleus of Purkinje cells, but not in the cytoplasm (Figure 3). Furthermore, we found that α1ACT decreased as the gene dosage increased. These results are consistent with the notion that the extended polyQ tract perturbed α1ACT expression in the nucleus by inhibition of nuclear translocation or other mechanisms. In addition, we found that mRNA and protein levels of TAF1 and BTG1 are also dependent on the gene dosage and well correlated with α1ACT expression. Our findings are consistent and complementary with the previous findings (Kordasiewicz et al., 2006; Du et al., 2013), supporting the hypothesis that polyQ-bearing α1ACT is involved in the pathogenesis.

Exploration of Unknown SCA6 Phenotypes for Pathogenic Investigation and Drug Screening

The patient Purkinje cells enable to explore unknown phenotypes before the disease onset. Findings brought by this exploration would be the basis for the mechanistic investigation of pathogenesis and for drug discovery in the future (Inoue et al., 2014; Watson et al., 2015). We searched for phenotypes specific to SCA6 Purkinje cells. SCA6 cells, but not control cells, show vulnerability to depletion of T3 as shrinkage of dendrites and decrease in cell number. Thus, we succeeded in construction of a T3 depletion-elicited SCA6 disease model. Although a causal relationship between T3 and SCA6 has not been reported, there are many reports (e.g., Barnard et al., 1971) that hypothyroidism in adult human is often accompanied by cerebellar ataxia and cerebellar atrophy, which can be reversibly improved with T3 treatment. Further studies on the hypothyroidism would provide information on the pathogenesis.

We found that TRH and Riluzole were effective to suppress the T3-dependent morphological changes. TRH in the hypothalamus stimulates the release of the thyroid stimulating hormone (TSH) from the pituitary gland, and TSH in turn stimulates the production of the thyroid hormone in the thyroid gland. However, it is unknown how TRH treatment suppressed the T3-dependent phenotypes in this in vitro model. Intriguingly, TRH receptors are expressed in many neurons including Purkinje cells and involved in the release of various neurotransmitters (Shibusawa et al., 2008). TRH shows a protective effect against death of motor

Figure 3. Decreased Expression of α1ACT and Its Target Molecules in SCA6 Purkinje Cells

(A) Scheme for Cav2.1 C-terminal domain (α1ACT) containing polyglutamine tract. α1ACT translated from the bicistronic transcript is translocated to the nucleus and upregulates the transcription of *TAF1* and *BTG1* (Du et al., 2013).

(B–G) Immunostaining of control (201B7) (B and E), heterozygous (SCD166-2-3) (C and F), and homozygous (SCD162-17-2) (D and G) Purkinje cells on days 75–80 for CALBINDIN (green), α1ACT (white), TAF1 (red in B–D), and BTG1 (red in E–G). Nuclear staining was overlaid (left columns). The white and cyan dotted lines encircle the soma and the nucleus, respectively. The scale bars represent 20 μm for low power images and 10 μm for magnified images.

(H–J) Relative fluorescence intensity of α1ACT (H), TAF1 (I), and BTG1 (J) normalized with the average of control values.

(K and L) Amounts of *TAF1* (K) and *BTG1* (L) mRNAs on day 75 estimated by qPCR.

Each bar represents mean ± SD from independent experiments ($n \geq 3$). *$p < 0.05$, **$p < 0.01$, and ***$p < 0.001$. See also Figure S3.

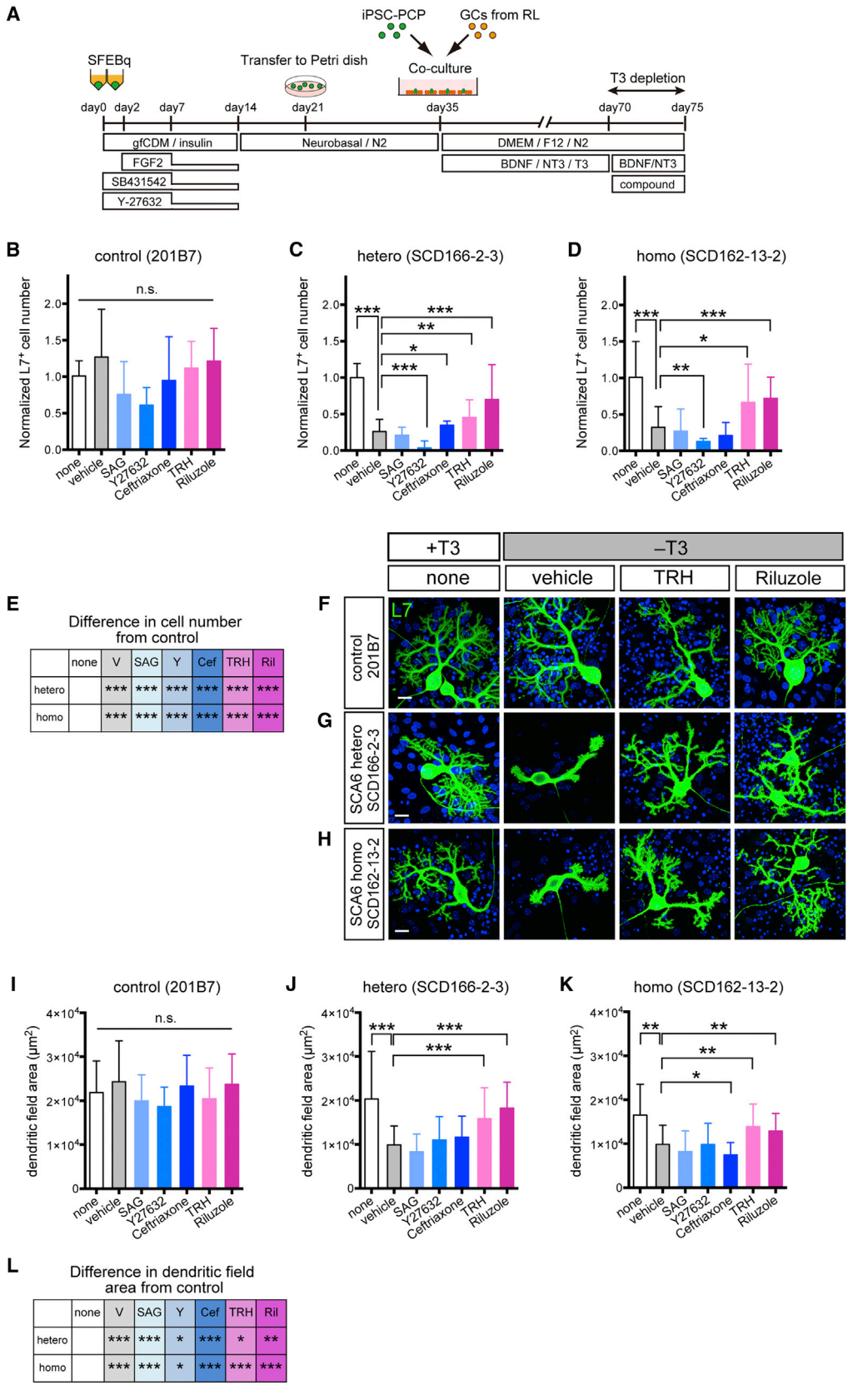

	none	V	SAG	Y	Cef	TRH	Ril
hetero		***	***	***	***	***	***
homo		***	***	***	***	***	***

	none	V	SAG	Y	Cef	TRH	Ril
hetero		***	***	*	***	*	**
homo		***	***	*	***	***	***

(legend on next page)

neurons derived from spinal muscular atrophy-specific iPSCs (Ohuchi et al., 2016). Clinically, TRH and its derivatives are used for treating cerebellar ataxia despite its marginal effects in SCA patients.

We also found that Riluzole suppressed the T3-depletion-dependent phenotypes. This finding is compatible with a clinical finding that Riluzole treatment has a positive effect on SCA patients (Romano et al., 2015). It was reported that neuronal excitation induced aggregation of the causative gene products in neurons from Machado-Joseph disease (SCA3) patients (Koch et al., 2011). However, ceftriaxone, an antibiotic agent that alleviates neuronal toxicity by promoting synaptic glutamate clearance and reduction of calcium influx (Maltecca et al., 2015), did not enhance the survival of SCA6 Purkinje cells (Figures 4B–4E, 4I–4L, and S4A–S4L). Taken together, we speculated inhibiting glutamate-independent neuronal excitation might contribute to the positive effect of Riluzole. Further pharmacological analysis would be necessary to reveal the mechanisms on the actions of both TRH and Riluzole.

EXPERIMENTAL PROCEDURES

iPSC Generation

DF- and PBMC-derived iPSCs were generated as described previously (Takahashi et al., 2007; Nakagawa et al., 2008; Okita et al., 2011) (See also Supplemental Experimental Procedures). The 201B7 and 253G1 control iPSCs were kindly provided by Dr. Yamanaka.

Microarray Analysis

Total RNA from DF as a control was commercially available (Cell Applications). Cy3-labeled RNA samples were hybridized with SurePrint G3 Human 8x60K v3 and scanned with the Agilent SureScan Microarray Scanner (G2600D, Agilent Technologies). The data were analyzed with Feature Extraction software (ver. 11.5.1.1, Agilent) and Subio Platform (ver. 1.19.4941, Subio).

Compound

iPSC-derived Purkinje cells were cultured in the cerebellar maturation medium (see Supplemental Experimental Procedures) without T3 for 5 days from culture day 70. Each compound was incubated in medium containing 10 μM CHIR99021 (Stemgent), 1 μM SAG (Enzo), 1 μM human TRH (OriGene), 100 μM ceftriaxone (TCI), 100 nM Riluzole (TCI), or 10 μM Y-27632 (Wako). To test responses for cellular stresses, tunicamycin (Sigma), bafilomycin A1 (Sigma), or MG132 (Cell Signaling) was used.

Intensity Quantification

Morphology and fluorescent intensity were analyzed with ImageJ (ver. 1.49, NIH). An average fluorescence intensity of a background-subtracted image was calculated within the region of interest for each sample. The values were normalized with an average intensity of controls.

Statistical Analysis

All data, shown as mean ± SD obtained from independent experiments ($n \geq 3$), were statistically analyzed with PRISM (GraphPad, ver. 6). Significance was tested with unpaired Student's t test for two-group comparisons or one-way ANOVA with Tukey-Kramer post hoc test.

ACCESSION NUMBERS

The accession numbers for microarray data reported in this paper are GEO: GSE85347 (gene-expression comparison iPSCs and hESCs) and GEO: GSE85348 (gene-expression comparison control and SCA6 neural progenitors).

SUPPLEMENTAL INFORMATION

Supplemental Information includes Supplemental Experimental Procedures, four figures, and one table and can be found with this article online at http://dx.doi.org/10.1016/j.celrep.2016.10.026.

AUTHOR CONTRIBUTIONS

K.M. conceived and supervised this project. K.M. and Y.I. performed the main body of experiments and data analysis. Y.I. performed the experiments as a visiting scientist of RIKEN. A.N. and H. Kitajima performed the experiments. H. Kawakami and H.I. provided patient samples and contributed to analysis with SCA-derived cells. K.M., Y.I., and H.I. wrote the manuscript. Y.S. designed this project. All authors read and approved the final manuscript.

ACKNOWLEDGMENTS

We thank Masayo Fujiwara, Ryo Yoshida, and Yuko Takeuchi for technical assistance; Masahiko Watanabe for kindly providing Cav2.1 antibody; and Kouichi Hashimoto and Daijiro Konno for invaluable comments. This work was supported by the Program for Intractable Disease Research Utilizing Disease-Specific iPS Cells from the Japan Science and Technology (JST) and Japan Agency for Medical Research and Development (AMED) (K.M., Y.S., and H.I.) and JSPS KAKENHI (K.M., 15K07089 and H. Kawakami, 26242085).

Received: April 23, 2016
Revised: August 15, 2016
Accepted: October 7, 2016
Published: November 1, 2016

REFERENCES

Barnard, R.O., Campbell, M.J., and McDonald, W.I. (1971). Pathological findings in a case of hypothyroidism with ataxia. J. Neurol. Neurosurg. Psychiatry *34*, 755–760.

Craig, P.J., McAinsh, A.D., McCormack, A.L., Smith, W., Beattie, R.E., Priestley, J.V., Yip, J.L.Y., Averill, S., Longbottom, E.R., and Volsen, S.G. (1998). Distribution of the voltage-dependent calcium channel α(1A) subunit throughout the mature rat brain and its relationship to neurotransmitter pathways. J. Comp. Neurol. *397*, 251–267.

Du, X., Wang, J., Zhu, H., Rinaldo, L., Lamar, K.M., Palmenberg, A.C., Hansel, C., and Gomez, C.M. (2013). Second cistron in *CACNA1A* gene encodes a transcription factor mediating cerebellar development and SCA6. Cell *154*, 118–133.

Figure 4. Degeneration of Dendrites in SCA6 Purkinje Cells by Nutrient Depletion and Its Suppression by Drug Treatments

(A) Time schedule for T3 depletion and compound treatment.

(B–D) Normalized numbers of $L7^+$ Purkinje cells from control (201B7) (B), heterozygous (SCD166-2-3) (C), and homozygous (SCD162-13-2) (D) iPSCs.

(E) Comparison of the cell numbers among the genotypes. The asterisks represent a significant different from the control.

(F–H) High-magnification images of $L7^+$ Purkinje cells (green) derived from control (F), heterozygous (G), and homozygous (H) iPSCs on culture day 75 in the presence or absence of T3 and with or without additional compounds. The scale bars represent 200 μm.

(I–K) Dendritic field area of control (I), heterozygous (J), and homozygous (K) Purkinje cells on day 75.

(L) Comparison of the dendritic field areas among the genotypes. The asterisks represent a significant difference from the control.

Each bar represents mean ± SD obtained from independent experiments ($n \geq 3$). *$p < 0.05$, **$p < 0.01$, ***$p < 0.001$. n.s., not significant. See also Figure S4.

Heuer, H., and Mason, C.A. (2003). Thyroid hormone induces cerebellar Purkinje cell dendritic development via the thyroid hormone receptor α1. J. Neurosci. *23*, 10604–10612.

Indriati, D.W., Kamasawa, N., Matsui, K., Meredith, A.L., Watanabe, M., and Shigemoto, R. (2013). Quantitative localization of Cav2.1 (P/Q-type) voltage-dependent calcium channels in Purkinje cells: somatodendritic gradient and distinct somatic coclustering with calcium-activated potassium channels. J. Neurosci. *33*, 3668–3678.

Inoue, H., Nagata, N., Kurokawa, H., and Yamanaka, S. (2014). iPS cells: a game changer for future medicine. EMBO J. *33*, 409–417.

Ishikawa, K., Tanaka, H., Saito, M., Ohkoshi, N., Fujita, T., Yoshizawa, K., Ikeuchi, T., Watanabe, M., Hayashi, A., Takiyama, Y., et al. (1997). Japanese families with autosomal dominant pure cerebellar ataxia map to chromosome 19p13.1-p13.2 and are strongly associated with mild CAG expansions in the spinocerebellar ataxia type 6 gene in chromosome 19p13.1. Am. J. Hum. Genet. *61*, 336–346.

Ishikawa, K., Fujigasaki, H., Saegusa, H., Ohwada, K., Fujita, T., Iwamoto, H., Komatsuzaki, Y., Toru, S., Toriyama, H., Watanabe, M., et al. (1999). Abundant expression and cytoplasmic aggregations of [α]1A voltage-dependent calcium channel protein associated with neurodegeneration in spinocerebellar ataxia type 6. Hum. Mol. Genet. *8*, 1185–1193.

Koch, P., Breuer, P., Peitz, M., Jungverdorben, J., Kesavan, J., Poppe, D., Doerr, J., Ladewig, J., Mertens, J., Tüting, T., et al. (2011). Excitation-induced ataxin-3 aggregation in neurons from patients with Machado-Joseph disease. Nature *480*, 543–546.

Kordasiewicz, H.B., Thompson, R.M., Clark, H.B., and Gomez, C.M. (2006). C-termini of P/Q-type Ca^{2+} channel α1A subunits translocate to nuclei and promote polyglutamine-mediated toxicity. Hum. Mol. Genet. *15*, 1587–1599.

Leto, K., Arancillo, M., Becker, E.B.E., Buffo, A., Chiang, C., Ding, B., Dobyns, W.B., Dusart, I., Haldipur, P., Hatten, M.E., et al. (2015). Consensus paper: Cerebellar development. Cerebellum. http://dx.doi.org/10.1007/s12311-015-0724-2.

Maltecca, F., Baseggio, E., Consolato, F., Mazza, D., Podini, P., Young, S.M., Jr., Drago, I., Bahr, B.A., Puliti, A., Codazzi, F., et al. (2015). Purkinje neuron Ca^{2+} influx reduction rescues ataxia in SCA28 model. J. Clin. Invest. *125*, 263–274.

Matilla-Dueñas, A., Ashizawa, T., Brice, A., Magri, S., McFarland, K.N., Pandolfo, M., Pulst, S.M., Riess, O., Rubinsztein, D.C., Schmidt, J., et al. (2014). Consensus paper: pathological mechanisms underlying neurodegeneration in spinocerebellar ataxias. Cerebellum *13*, 269–302.

Matsuyama, Z., Kawakami, H., Maruyama, H., Izumi, Y., Komure, O., Udaka, F., Kameyama, M., Nishio, T., Kuroda, Y., Nishimura, M., and Nakamura, S. (1997). Molecular features of the CAG repeats of spinocerebellar ataxia 6 (SCA6). Hum. Mol. Genet. *6*, 1283–1287.

Miyazaki, Y., Du, X., Muramatsu, S., and Gomez, C.M. (2016). An miRNA-mediated therapy for SCA6 blocks IRES-driven translation of the *CACNA1A* second cistron. Sci. Transl. Med. *8*, 347ra94.

Morino, H., Matsuda, Y., Muguruma, K., Miyamoto, R., Ohsawa, R., Ohtake, T., Otobe, R., Watanabe, M., Maruyama, H., Hashimoto, K., and Kawakami, H. (2015). A mutation in the low voltage-gated calcium channel *CACNA1G* alters the physiological properties of the channel, causing spinocerebellar ataxia. Mol. Brain *8*, 89.

Muguruma, K., Nishiyama, A., Ono, Y., Miyawaki, H., Mizuhara, E., Hori, S., Kakizuka, A., Obata, K., Yanagawa, Y., Hirano, T., and Sasai, Y. (2010). Ontogeny-recapitulating generation and tissue integration of ES cell-derived Purkinje cells. Nat. Neurosci. *13*, 1171–1180.

Muguruma, K., Nishiyama, A., Kawakami, H., Hashimoto, K., and Sasai, Y. (2015). Self-organization of polarized cerebellar tissue in 3D culture of human pluripotent stem cells. Cell Rep. *10*, 537–550.

Nakagawa, M., Koyanagi, M., Tanabe, K., Takahashi, K., Ichisaka, T., Aoi, T., Okita, K., Mochiduki, Y., Takizawa, N., and Yamanaka, S. (2008). Generation of induced pluripotent stem cells without Myc from mouse and human fibroblasts. Nat. Biotechnol. *26*, 101–106.

Ohuchi, K., Funato, M., Kato, Z., Seki, J., Kawase, C., Tamai, Y., Ono, Y., Nagahara, Y., Noda, Y., Kameyama, T., et al. (2016). Established stem cell model of spinal muscular atrophy is applicable in the evaluation of the efficacy od thyrotropin-releasing hormone analog. Stem Cells Transl. Med. *5*, 152–163.

Okita, K., Matsumura, Y., Sato, Y., Okada, A., Morizane, A., Okamoto, S., Hong, H., Nakagawa, M., Tanabe, K., Tezuka, K., et al. (2011). A more efficient method to generate integration-free human iPS cells. Nat. Methods *8*, 409–412.

Okita, K., Yamakawa, T., Matsumura, Y., Sato, Y., Amano, N., Watanabe, A., Goshima, N., and Yamanaka, S. (2013). An efficient nonviral method to generate integration-free human-induced pluripotent stem cells from cord blood and peripheral blood cells. Stem Cells *31*, 458–466.

Romano, S., Coarelli, G., Marcotulli, C., Leonardi, L., Piccolo, F., Spadaro, M., Frontali, M., Ferraldeschi, M., Vulpiani, M.C., Ponzelli, F., et al. (2015). Riluzole in patients with hereditary cerebellar ataxia: a randomised, double-blind, placebo-controlled trial. Lancet Neurol. *14*, 985–991.

Rüb, U., Schöls, L., Paulson, H., Auburger, G., Kermer, P., Jen, J.C., Seidel, K., Korf, H.W., and Deller, T. (2013). Clinical features, neurogenetics and neuropathology of the polyglutamine spinocerebellar ataxias type 1, 2, 3, 6 and 7. Prog. Neurobiol. *104*, 38–66.

Sasai, Y. (2013). Next-generation regenerative medicine: organogenesis from stem cells in 3D culture. Cell Stem Cell *12*, 520–530.

Shibusawa, N., Hashimoto, K., and Yamada, M. (2008). Thyrotropin-releasing hormone (TRH) in the cerebellum. Cerebellum *7*, 84–95.

Takahashi, K., Tanabe, K., Ohnuki, M., Narita, M., Ichisaka, T., Tomoda, K., and Yamanaka, S. (2007). Induction of pluripotent stem cells from adult human fibroblasts by defined factors. Cell *131*, 861–872.

Unno, T., Wakamori, M., Koike, M., Uchiyama, Y., Ishikawa, K., Kubota, H., Yoshida, T., Sasakawa, H., Peters, C., Mizusawa, H., and Watase, K. (2012). Development of Purkinje cell degeneration in a knockin mouse model reveals lysosomal involvement in the pathogenesis of SCA6. Proc. Natl. Acad. Sci. USA *109*, 17693–17698.

Watson, L.M., Wong, M.M.K., and Becker, E.B.E. (2015). Induced pluripotent stem cell technology for modelling and therapy of cerebellar ataxia. Open Biol. *5*, 150056.

Westenbroek, R.E., Sakurai, T., Elliott, E.M., Hell, J.W., Starr, T.V.B., Snutch, T.P., and Catterall, W.A. (1995). Immunochemical identification and subcellular distribution of the α 1A subunits of brain calcium channels. J. Neurosci. *15*, 6403–6418.

Yang, Q., Hashizume, Y., Yoshida, M., Wang, Y., Goto, Y., Mitsuma, N., Ishikawa, K., and Mizusawa, H. (2000). Morphological Purkinje cell changes in spinocerebellar ataxia type 6. Acta Neuropathol. *100*, 371–376.

Zhuchenko, O., Bailey, J., Bonnen, P., Ashizawa, T., Stockton, D.W., Amos, C., Dobyns, W.B., Subramony, S.H., Zoghbi, H.Y., and Lee, C.C. (1997). Autosomal dominant cerebellar ataxia (SCA6) associated with small polyglutamine expansions in the α 1A-voltage-dependent calcium channel. Nat. Genet. *15*, 62–69.